AD-A145 111    ON THE CALCULATING MODELS OF PERMANENT MAGNETS(U)    1/1
FOREIGN TECHNOLOGY DIV WRIGHT-PATTERSON AFB OH  S YUSHI
26 JUL 84 FTD-ID(RS)T-0718-84

UNCLASSIFIED    F/G 12/1    NL

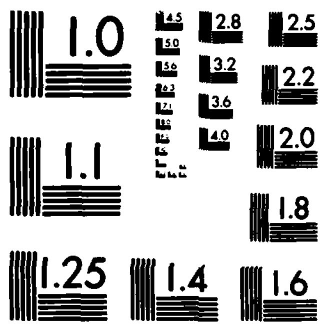


MICROCOPY RESOLUTION TEST CHART
NATIONAL BUREAU OF STANDARDS-1963-A

FTD-ID(RS)T-0718-84

# FOREIGN TECHNOLOGY DIVISION

AIR FORCE SYSTEMS COMMAND

## ON THE CALCULATING MODELS OF PERMANENT MAGNETS

by

Sun Yushi

FOREIGN TECHNOLOGY DIVISION



Approved for public release;
distribution unlimited.

# EDITED TRANSLATION

FTD-ID(RS)T-0718-84 26 July 1984

MICROFICHE NR: FTD-84-C-000743

ON THE CALCULATING MODELS OF PERMANENT MAGNETS

By: Sun Yushi

English pages: 11

Source: Dianzi Xuebao, Vol. 10, Nr. 5, September-October 1982, pp. 86-89

Country of origin: China
Translated by: SCITRAN
F33657-81-D-0263
Requester: FTD/TQTD
Approved for public release; distribution unlimited.

## GRAPHICS DISCLAIMER

All figures, graphics, tables, equations, etc. merged into this translation were extracted from the best quality copy available.



A-1

718-84

# On The Calculating Models of Permanent Magnets ① /86

Sun Yushi ②

(Nanjing Aeronautical Institute) ②

[Abstract] Two improvements were proposed for two calculating models for permanent magnets (the scalar potential model and the vector potential model) in this paper. Volumetric density was replaced by an appropriate hypothetical surface density of magnetic monopole (or surface bound current density) which did not vary with the operating point. The definition of magnetic reluctivity was correspondingly modified in the vector potential model to simplify the calculation and computer program. The improved models have been proven through computation and experiments.

## I. Introduction

The widely used calculating models for permanent magnets in engineering include the scalar potential model[1] (Model I hereafter) and the vector potential model [1,2] (Model II hereafter).

According to Model I, a permanent magnet is considered to be comprised of distributed hypothetic magnetic monopoles (the volumetric magnetic monopole density is $\rho_{m0}$) and various anistropic magnetic conductors. Therefore, a permanent magnetic field is expressed by the following quasi-Poisson equation.

$$\mathrm{div}\mu\,\mathrm{grad}U = -\rho_{m0} \tag{1}$$

and

$$\rho_{m0} = -\mu_0 \mathrm{div}M_0 \tag{2}$$

where U is the scalar magnetic potential, $\mu_0$ is the magnetic permitivity in vacuum, and $M_0$ is the magnetization vector in the permanent magnetic when the magnetic field strength H is zero. ③

① received in October 1980, revised in December 1981
② Sun Yushi (Nanjing Aeronautical Institute)
③ For ease of expression, rectangular coordinates were used throughout this work. It was also assumed that the original permament magnet and magnetizing directions were along the Z-axis.

$$M_3 = \begin{bmatrix} M_{3q} \\ M_{3d} \\ M_{0p} \end{bmatrix} = \frac{1}{\mu_3} \begin{bmatrix} B_{3q} \\ B_{3d} \\ B_{3p} \end{bmatrix} \qquad \text{(A)}$$

The definitions of $B_{0q}$ and $B_{0p}$ are shown in Figure 1. $\mu$ is the magnetic permitivity matrix of the permanent magnet:

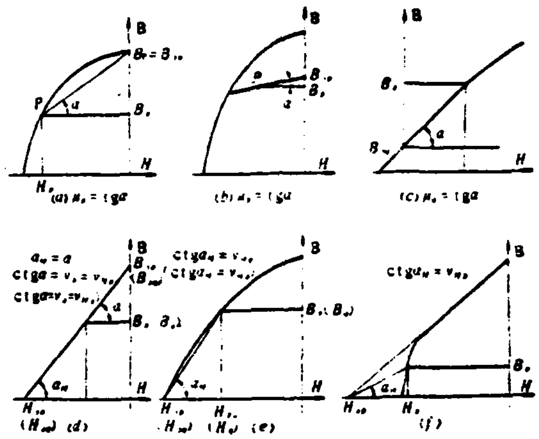


Figure 1. Geometric Significance of Several Magnetic Conductivity (or Magnetic Reluctivity)

a. operating point on demagnetization line ($\mu_p = 1/\nu_p$);
b. operating point on restoration line ($\mu_p = 1/\nu_p$);
c. operating point perpendicular to magnetizing direction ($\mu_q = 1/\nu_q$);
d. linear condition, $\nu_{Hp} = \nu_p$ ($\nu_{Hq} = \nu_q$);
e. $\nu_{Hp}$ non-linear condition ($\nu_{Hq}$);
f. $\nu_{Hp}$ in calculating example 2.

$$\mu = \begin{bmatrix} \mu_q & 0 & 0 \\ 0 & \mu_q & 0 \\ 0 & 0 & \mu_p \end{bmatrix} \tag{B}$$

Furthermore

$$\mu_p = (B_p - B_{0p})/H_p \tag{3}$$

$$\mu_q = (B_q - B_{0q})/H_q \tag{4}$$

According to Model II, a permanent magnet is considered to be comprised of bound currents (the volumetric current density is $J_{mo}$) and various anisotropic magnetic conductors. Therefore, a permanent magnetic field (when a macroscopic current density J is present) satisfies the following equation

$$\mathrm{rot}(\nu\,\mathrm{rot}A) = J_{mo} + J \tag{5}$$

$$J_{mo} = \mu_0\,\mathrm{rot}(\nu M_0) \tag{6}$$

where A is the vector magnetic potential and $\nu$ is the apparent magnetic reluctivity matrix, and

$$\nu = \begin{bmatrix} \nu_q & 0 & 0 \\ 0 & \nu_q & 0 \\ 0 & 0 & \nu_p \end{bmatrix}, \quad \nu_q = \frac{1}{\mu_q},$$
$$\nu_p = \frac{1}{\mu_p} \tag{C}$$

In the two models mentioned above, $\mu_q$ or $\nu_q$ cannot be found from experimental data. Furthermore, their selection

is not consistent. Frequently, a certain parameter in the magnetization direction of the permanent magnet is made to be $\mu_q$.

The author made the following modifications through supplementing derivation and reorganization of equations (1) and (2). The expressions for surface monopole density and bound surface current were supplemented. In Model II, the bound volumetric current could be avoided in ordinary conditions through an appropriate modification of magnetic reluctivity. Furthermore, bound surface current was made to be independent of the non-linear coefficient matrix to simplify the calculating process. In addition, objections were raised against the determination of magnetic permitivity $\mu_q$ (or magnetic reluctivity) perpendicular to the direction of magnetization in the original model. It was pointed out that $\mu_q$ must be obtained experimentally.

II. Modification of Model II

The characteristic equations (3) and (4) for Figure 1 (a,b,c) can be expressed by the following matrix equation:

$$H=\nu(B-\mu_0 M_0) \tag{7}$$

By taking the curl on both sides of eq. (7), we got equations (5) and (6). On this basis, the boundary conditions of the medium with macroscopic surface current were compared to those without such current(surface bound current density is considered as macroscopic surface current density in Model II). An expression for the surface bound current density $j_{mo}$ could be derived from the tangential component of H.

$$j_{m0}=\mu_0(\nu M_0)\times n \tag{8}$$

where n is a unit vector in the normal direction along the surface of the permanent magnet. From equations (6) and (8) one can see that $J_{mo}$ and $j_{mo}$ are both directly related to the vector $\mu_0(\nu M_0)$.

If $\mu_0$ $(\nu M_0)$ is a constant, then $J_{m0}$ is always zero [4] and $j_{m0}$ is a constant. However, $\nu$ usually varies with the operating point for a permanent magnet. Therefore, $\mu_0$ $(\nu M_0)$ cannot be a constant. Hence, in Model II which is expressed by equations (5), (6) and (8). It is inavoidable to have $J_{m0}$ present and $j_{m0}$ varying with the operating point.

There were enough reasons to express the characteristics of a permanent magnet [see Figure 1 (d, e)] by another matrix equation i.e.,

$$H = \nu_H B - H_0. \tag{9}$$

where $\nu_H$ is the equivalent magnetic reluctivity matrix of the permanent magnet. Furthermore,

$$\left.\begin{aligned} \nu_H &= \begin{bmatrix} \nu_{Hr} & 0 & 0 \\ 0 & \nu_{Hz} & 0 \\ 0 & 0 & \nu_{H\theta} \end{bmatrix} \\ \nu_{Hr} &= (H_r - H_{0r})/B_r \\ \nu_{Hz} &= (H_z - H_{0z})/B_z \end{aligned}\right\} \tag{10}$$

$H_0$ is the equivalent coercivity vector and

$$H_0 = \begin{bmatrix} -H_{0r} \\ -H_{0z} \\ -H_{0\theta} \end{bmatrix} \tag{D}$$

Obviously, equation (9) is equivalent to (7). Furthermore, under a linear condition, $\nu_H = \nu$ and $H_0 = \mu_0(\nu M_0)$. After treating equation (7) with the same treatment as for equation

4 This conclusion is applicable to a permanent magnet magnetized in the z direction and along a radial direction. However, it is not suited for circumferential magnetization.

(9), the overall expressions for the improved Model II were:

$$\left.\begin{array}{l} \mathrm{rot}(\nu_H \mathrm{rot} A) = J_{mH} + J \\ J_{mH} = \mathrm{rot} H_c \\ j_{mH} = H_c \times n \end{array}\right\} \qquad (11)$$

From the magnetization direction it is possible to determine that $J_{mH}$ is zero in most cases (such as magnetizing along z-axis or radially). It is a constant vector only when it is magnetized circumferentially. However, $j_{mH}$ is invariantly a constant vector.

From the equivalence of mathematical expressions, the selection of $H_{0p}$ and $H_{0q}$ is arbitrary, in principle. However, whether the choice is appropriate will affect the converging rate of the computation. For example, in example 2 in this paper, when the permanent magnet is samarium-praseodymium-cobalt [its characteristic is shown in Figure 1 (f)], the operating region of the permanent magnetic is mainly in the linear portion of the curve. Therefore, the fluctuation of $\nu_{Hp}$ can be minimized in iterations by choosing $H_{0p}$ at the intercept of the extension of the linear section of the characteristic curve with the horizontal coordinate obtaining the fastest convergence.

III. Supplement to Model I

From equation (7), the boundary conditions of the media with a hypothetic surface magnetic monopole density were compared to those without it. The expression for the hypothetical surface magnetic monopole density on a permanent magnet could be derived by using the normal component of B:

$$\sigma_{m0} = \mu_0 M_0 \cdot n \qquad (12)$$

From equation (2) and (12) one can see that both $\sigma_{m0}$ and $\rho_{m0}$ are unrelated to $\mu$. Therefore, when $M_0$ is a constant, $\rho_{m0}$ in most cases is invariantly zero. It is a constant only when /88
the magnetization is along a radial direction $Z.\sigma_{m0}$, however, is always a constant. This shows that in most cases only the

effect of surface magnetic monopole must be considered. Volumetric magnetic monopole does not have to be taken into account.

## IV. Magnetic Permitivity in Perpendicular Direction

The author conducted experiments on two batches of specimens made primarily of AlNiCo-5 and the typical data and curves are shown in Table 1 and Figure 2. The experimental results explained the following three situations. $\mu_q$ is an independent parameter different from parameters such as $\mu_{rec}$, $K_r$, and $\mu_p$ which are determined by the magnetization direction. Within the range of $H_q < 0.5{}_BH_C$, $\mu_q$ is nearly a constant. When $H_q$ is not large, the hysteresis of the $B_q$-$H_q$ curve is very small and $M_{0q}$ can approximately be considered as zero for a permanent magnet. $\mu_q$ is not apparently related to the magnetic state in the magnetization condition. Therefore, $\mu_q$ should be obtained experimentally.

Table 1. Average Values of Important Parameters of the First Batch Samples (Seven) in Magnetization and Perpendicular Directions

| $B_r$ (T) | ${}_BH_C$ (A/m) | $\mu_{rec}$ ($10^{-6}$H/m) | $k_r$ ($10^{-6}$H/m) | $\mu_q$ ($10^{-6}$H.m) |
|---|---|---|---|---|
| 1.298 | $4.84 \times 10^4$ | 4.76 | 3.87 | 9.58 |

Table 2. Typical $B_q$-$H_q$ Characteristic Curve of a AlNiCo-5 Specimen (reproduced according to the curve measured)

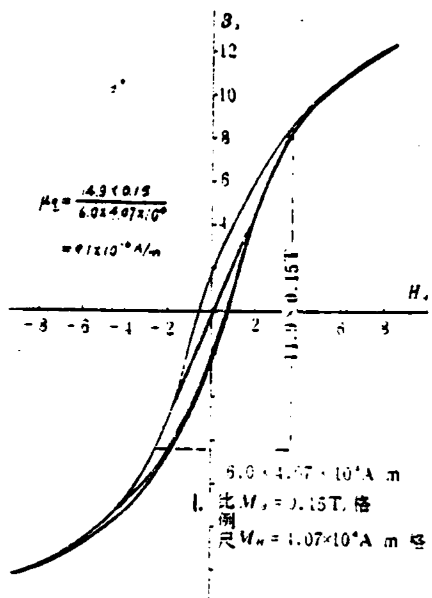


1. scale $M_B$ = 0.15T/div. $M_H$ = 4.07 x $10^4$ A/m/dov.

V. Experimental Proof

Example 1. A square cross-section permanent magnetic bar was used to prove the expression for surface magnetic monopole in Model I. Furthermore, the calculated curve of $B_y$ and the measured points are shown in Figure 3.

The finite difference method was used in theoretical calculation. A coarse computation was carried out in a relatively large area (nodal points 27 x 27 x 26 = 18954). Then, a fine calculation was performed in a correspondingly reduced area (nodal points 26 x 26 x 25 = 16900). The demagnetization and $\mu_q$ used in the computation were all

actually measured numerical values.

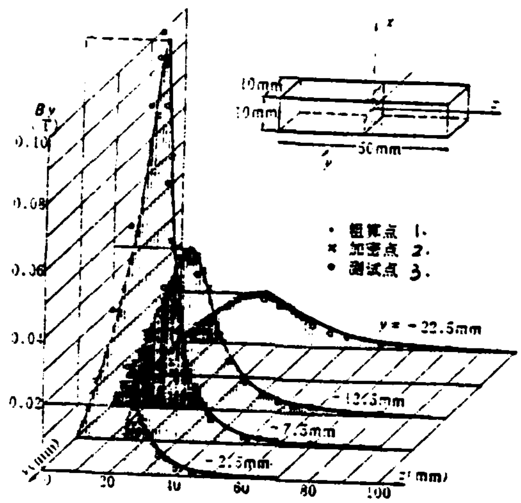


Figure 3. Calculated Curves and Distribution of Measured Points ($B_y$) in Example 1.

The measuring instrument was a Hall effect gaussmeter. From Figure 3 one can see that the theory coincides with practice. Example2. A permanent magnetic ring (made of YX-30) in the radial direction was used to verify the improved Model II (see Figure 4). For ease of comparison, calculated results obtained based on Model I are also given in Figure 4 (the finite difference method was used for Model I with 95 x 34 = 3230 nodal points).

Both the finite difference method and the finite element method were used in the verification process (the grid division of the finite difference method was the same as that in Model I, and the nodal points were 164 for the finite element method). The results are basically in agreement with those in Model I.

In addition, the permanent magnetic ring was used to verify the accelerated convergence effect of the improved Model II. The permanent magnet shows a non-linear character at below 0.7T. The selection of $H_{0p}$ and $\nu_{Hp}$ is shown in Figure 1 (f). The original and improved models were used to calculate the potential, and the under relaxation iteration method was used to correct the non-linear coefficients $\nu_p$ and $\nu_{Hp}$. The converging situations using various under-relaxation factors $\omega$ are listed in Table 2. On can see that the converging rate is greatly improved after Model II was improved.

/89

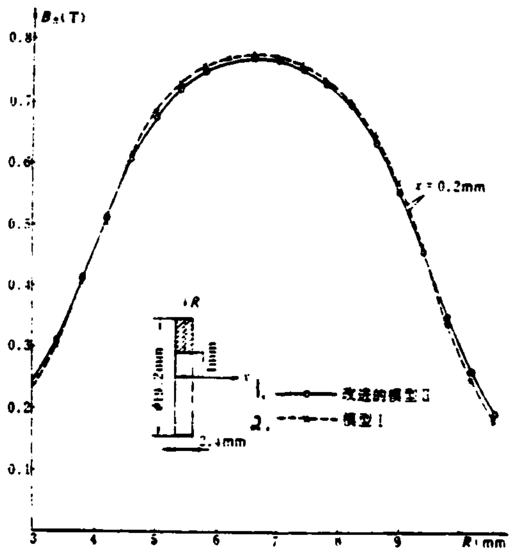


Figure 4. Comparison of Results Obtained Using Finite Difference Method with Model II to Model I ($B_R$ portion)
1. improved Model II     2. Model I

Table 2. Comparison of Convergence Under Various W

| 迭代次数 1. / 模型 2. \ ω | 1.0 | 0.6 | 0.3 | 0.15 | 0.1 |
|---|---|---|---|---|---|
| 3. 原模型 II | 5 不收敛 | 6 不收敛 | 7 不收敛 | 8 不收敛 | 42 |
| 4. 改进模型 II | 4 | 7 | 11 | 17 | 9 (未算) |

1. number iteration
2. model
3. original Model II
4. modified Model II
5. non-convergence
6. non-convergence
7. non-convergence
8. non-convergence
9. (not calculated)

Acknowledgement. The author expresses gratitude towards his teacher Ye Erhua who assisted in the mathematical aspect, and comrades Mei Junwei, Zhao Zhonggang, Hu Jianren, and Jia Liuhai who helped in computation and measurement.

## References

[1] W.J. Harrold, IEEE Trans., Vol. MAG-8, 1972, p. 23.

[2] K.J. Binns, M.A. Jabbar and W.R. Barnard, PIEE Vol. 122, No. 12, 1975, p. 1377.

END

FILMED

9-84